

# Revisit the fundamental plane of black-hole activity from sub-Eddington to quiescent state

Ai-Jun Dong<sup>1,2</sup>, Qingwen Wu<sup>1\*</sup>

<sup>1</sup>*School of Physics, Huazhong University of Science and Technology, Wuhan 430074, China*

<sup>2</sup>*Department of Electron information Engineering, Chuzhou University, Chuzhou 23900, China*

30 March 2021

## ABSTRACT

It is very controversial whether radio–X-ray correlation as defined in low-hard state of X-ray binaries (XRBs) can extend to quiescent state (e.g., X-ray luminosity less than a critical value of  $L_{X,c} \sim 10^{-5.5} L_{\text{Edd}}$ ) or not. In this work, we collect a sample of XRBs and low luminosity active galactic nuclei (LLAGNs) with wide distribution of Eddington ratios ( $L_X/L_{\text{Edd}} \sim 10^{-9} - 10^{-3}$ ) to reexplore the fundamental plane between 5 GHz radio luminosity,  $L_R$ , 2–10 keV X-ray luminosity,  $L_X$ , and black hole (BH) mass,  $M_{\text{BH}}$ , namely  $\log L_R = \xi_X \log L_X + \xi_M \log M_{\text{BH}} + \text{constant}$ . For the whole sample, we confirm the former fundamental plane of Merloni et al. and Falcke et al. that  $\xi_X \sim 0.6$  and  $\xi_M \sim 0.8$  even after including more quiescent BHs. The quiescent BHs follow the fundamental plane very well, and, however, FR I radio galaxies follow a steeper track comparing other BH sources. After excluding FR Is, we investigate the fundamental plane for BHs in quiescent state with  $L_X < L_{X,c}$  and sub-Eddington BHs with  $L_X > L_{X,c}$  respectively, and both subsamples have a similar slope,  $\xi_X \sim 0.6$ , which support that quiescent BHs may behave similar to those in low-hard state. We further select two subsamples of AGNs with BH mass in a narrow range (FR Is with  $M_{\text{BH}} = 10^{8.8 \pm 0.4}$  and other LLAGNs with  $M_{\text{BH}} = 10^{8.0 \pm 0.4}$ ) to simulate the behavior of a single supermassive BH evolving from sub-Eddington to quiescent state. We find that the highly sub-Eddington sources with  $L_X/L_{\text{Edd}} \sim 10^{-6} - 10^{-9}$  still roughly stay on the extension of radio–X-ray correlation as defined by other sub-Eddington BHs. Our results are consistent with several recent observations in XRBs that the radio–X-ray correlation as defined in low-hard state can extend to highly sub-Eddington quiescent state.

**Key words:** accretion, accretion discs — black hole physics — ISM:jets and outflows — X-rays: binaries — methods:statistical

## 1 INTRODUCTION

Accreting black holes (BHs) are widely accepted to be the central engines powering most of emission from X-ray binaries (XRBs) and active galactic nuclei (AGNs), where the BH masses are around 3–20  $M_{\odot}$  in XRBs and  $10^5 - 10^{10} M_{\odot}$  in the center of every large galaxy. The putative intermediate BHs ( $10^2 - 10^4 M_{\odot}$ ) are still a matter of debate. XRBs are normally transient sources which display complex spectral and timing features during the outbursts, where three main states include high/soft (HS) state, low/hard (LH) state and intermediate state (or steep power-law state). The HS state is characterized by a strong thermal component and a weak power-law component, while the thermal component is weak and power-law component is dominant in LH state. The intermediate state is normally dominated by a steep power-law component (e.g., see McClintock & Remillard 2006 and Zhang 2013 for recent re-

views and references therein). It is much complex in AGNs, where statistical investigations suggest that the different types of AGNs can be unified with several parameters (e.g., orientation and radio loudness, Urry & Padovani 1995). Several works have tried to establish connections between the different states of XRBs and different types of AGNs, where low luminosity AGNs (LLAGNs) are analogs of the XRBs in LH state, RQ quasars are analogs of the XRBs in HS state, while AGNs with relativistic jets may correspond to the XRBs in intermediate state (e.g., Falcke et al. 2004 and Kording et al. 2006a).

The HS state of XRBs and bright AGNs are believed to be powered by a cold, optically thick, geometrically thin standard accretion disc (SSD; Shakura & Sunyaev 1973) that accompanied with some fraction of hot optically thin corona above and below the disc. However, SSD component is normally weak or absent in LH state and most of the radiation comes from the non-thermal power-law component that may come from the hot, optically thin, geometrically thick advection-dominated accretion flows

\* Corresponding author, E-mail: qwwu@hust.edu.cn

(ADAFs, also called radiatively inefficient accretion flows, RIAFs, Ichimaru 1977; Narayan & Yi 1994, 1995; Abramowicz et al. 1995; Wu & Cao 2006 and see Yuan & Narayan 2014 for a recent review and references therein). The anti- and positive correlations between hard X-ray index and Eddington ratio as found in both XRBs (e.g., Wu & Gu 2008) and AGNs (e.g., Wang et al. 2004; Shemmer et al. 2008; Gu & Cao 2009; Constantin et al. 2009) may support the transition of accretion modes (e.g., Cao 2009; Qiao & Liu 2013; Cao et al. 2014; Cao & Wang 2015).

The radio and X-ray correlation has long been studied in both XRBs and AGNs, which was used to explore the possible connection between jet and accretion disc (see Yuan et al. 2003; Liu & Wu 2013, for different opinion for the radio emission in quiescent supermassive BHs). The quasi-simultaneous radio and X-ray fluxes in LH state of XRBs roughly follow a universal non-linear correlation ( $F_R \propto F_X^b$ ,  $b \sim 0.5 - 0.7$ , Hannikainen et al. 1998; Corbel et al. 2003; Gallo et al. 2003; Corbel et al. 2013). Recently, more and more XRBs deviate from the universal correlations (e.g., Xue & Cui 2007; Cadolle Bel et al 2007; Soleri et al. 2010; Jonker et al. 2010; Coriat et al. 2011; Ratti et al. 2012) and form a different ‘outliers’ track with a much steeper radio–X-ray correlation ( $b \sim 1.4$  as initially found in H1743–322, Coriat et al. 2011). Cao et al. (2014) found that the X-ray spectral evolutions are different for the data points in the universal and ‘outliers’ tracks, which support that these two tracks may be regulated by radiatively inefficient and radiatively efficient accretion discs respectively (see also Coriat et al. 2011; Huang et al. 2014; Qiao & Liu 2015). It is the similar case in AGNs, where LLAGNs follow a shallower radio–X-ray correlation (e.g., the index  $b \sim 0.6$ , Wu et al. 2013) while bright AGNs normally follow a much steeper correlation (e.g.,  $b \sim 1.6$ , Dong et al. 2014; Panessa et al. 2015).

By taking into account the BH mass, the universal radio–X-ray correlation of  $F_R \propto F_X^{0.6}$  was extended to AGNs, which is called “fundamental plane” of BH activity (e.g., Merloni et al. 2003),

$$\log L_R = 0.60_{-0.11}^{+0.11} \log L_X + 0.78_{-0.09}^{+0.11} \log M_{\text{BH}} + 7.33_{-4.07}^{+4.05}, \quad (1)$$

where  $L_R$  is 5 GHz nuclear radio luminosity in unit of  $\text{erg s}^{-1}$ ,  $L_X$  is 2–10 keV nuclear X-ray luminosity in unit of  $\text{erg s}^{-1}$ , and  $M_{\text{BH}}$  is the BH mass in unit of  $M_{\odot}$  (see also Falcke et al. 2004; Wang et al. 2006; K rding et al. 2006b; Li et al. 2008; Yuan et al. 2009; G ltekin et al. 2009a; Plotkin et al. 2012). This fundamental plane is tightest for LH state of XRBs and sub-Eddington AGNs (K rding et al. 2006b). Both ‘outliers’ of XRBs and bright AGNs follow a steeper radio–X-ray correlation and a positive hard X-ray photon index–Eddington ratio correlation ( $\Gamma - L/L_{\text{Edd}}$ ), which is most possibly regulated by disk-corona model (Dong et al. 2014). Based on these similarities, Dong et al. (2014) proposed a new fundamental plane for radiatively efficient BHs,

$$\log L_R = 1.59_{-0.22}^{+0.28} \log L_X - 0.22_{-0.20}^{+0.19} \log M_{\text{BH}} - 28.97_{-0.45}^{+0.45}. \quad (2)$$

These two universal correlations of Merloni et al. (2003) and Dong et al. (2014) with much different slopes of  $\xi_X$  are most possibly regulated by radiatively inefficient and radiatively efficient BH sources respectively.

The nature of BHs in quiescent state remains an open issue. The anti-correlation between hard X-ray photon index and Eddington ratio ( $\Gamma - L_X/L_{\text{Edd}}$ ) are found for LH-state of BHs with  $L_X/L_{\text{Edd}} \lesssim 0.1\%$  (e.g., Wu & Gu 2008). However, this anti-correlation as found in LH state does not continue once the XRB enters quiescence, where  $\Gamma$  keeps roughly a constant when  $L_X/L_{\text{Edd}} \lesssim 10^{-5}$  (e.g., Plotkin et al. 2013, see also Yang et al. 2015 for possible evidence in AGNs). The physical reason is still

unclear, where Yang et al. (2015) proposed that the X-ray emission in quiescent state may be dominated by the jet and the value of  $\Gamma$  should keep as a constant while the X-ray emission dominantly come from ADAF in LH state. The spectral energy distribution (SED) modeling also preferred the pure jet model for these quiescent BHs (e.g., Xie et al. 2014; Plotkin et al. 2015). Yuan & Cui (2005) explored the universal correlation of  $F_R \propto F_X^{0.7}$  as found in LH state of XRBs based on ADAF-jet model and predicted that the radio–X-ray correlation will also deviate from that of LH state and will become steeper as  $F_R \propto F_X^{1.23}$  when the X-ray luminosity is lower than a critical luminosity ( $L_{X,c} \sim 10^{-6} - 10^{-5} L_{\text{Edd}}$ ), where both the radio and X-ray emission should dominantly come from the jet. Yuan et al. (2009)’s results seemed to support this prediction based on a small sample of LLAGNs with X-ray luminosity roughly below the critical value. However, several quiescent BH XRBs seem to challenge this prediction that they still follow the radio–X-ray correlation as defined in LH state very well and do not evidently deviate even for  $L_X < 10^{-8} L_{\text{Edd}}$  (Gallo et al. see 2006, 2014, for A0620-00 and XTE J1118+480 and see also Calvelo et al. 2010). Therefore, it is still unclear whether quiescent XRBs follow the radio–X-ray correlation as found in LH state of XRBs or not.

In recent years, more and more radio and X-ray observations were available for quiescent supermassive BHs in LLAGNs and the data also increased for XRBs in quiescent state. In this work, we aim to reexplore the radio–X-ray correlation and the fundamental plane for BH sources from sub-Eddington down to quiescent state by collecting more quiescent BHs. Throughout this work, we assume the following cosmology for AGNs:  $H_0 = 70 \text{ km s}^{-1} \text{ Mpc}^{-1}$ ,  $\Omega_0 = 0.27$  and  $\Omega_{\Lambda} = 0.73$ .

## 2 SAMPLE

For purpose of our work, we select the XRBs and LLAGNs from sub-Eddington to quiescent state, where we particularly include much more quiescent BHs compared former works. Yuan & Cui (2005) predicted that the X-ray emission should be dominated by jet and the radio–X-ray correlation will become steeper if the X-ray luminosity of BH systems is lower than a critical value through modeling the radio–X-ray correlation of XRBs in LH state with the ADAF-jet model. This critical X-ray luminosity is

$$\log \frac{L_{X,c}}{L_{\text{Edd}}} = -5.356 - 0.17 \log \frac{M_{\text{BH}}}{M_{\odot}}, \quad (3)$$

where the critical Eddington ratio is also roughly consistent with the change of hard X-ray spectral evolution from LH to quiescent state in XRBs (e.g.,  $L_X \lesssim 10^{-5.5} L_{\text{Edd}}$ , Plotkin et al. 2013). To separate the quiescent BHs from our samples, we simply use the criteria of equation (3).

For XRBs, we select three sources with fruitful simultaneous or quasi-simultaneous radio and X-ray observations with  $L_X \lesssim 10^{-3} L_{\text{Edd}}$  in LH state (GX 339-4, Cao et al. 2014; XTE J1118+480 and V404 Cyg, Fender et al. 2010 and references therein). Some LH-state XRBs that stay in ‘outliers’ track or have only few simultaneous observations are neglected. Five quiescent XRBs with simultaneous or quasi-simultaneous radio and X-ray observations were selected from literatures, which are XTE J1752-223 (Ratti et al. 2012), H1743-322 (Coriat et al. 2011), XTE J1118+480 (Gallo et al. 2014), A06200-00 and V404 Cyg (Fender et al. 2010). The radio luminosity at 5 GHz and X-ray luminosity in 2–10 keV band were adopted in our work, where the radio emission observed in different waveband is extrapolated to

**Table 1. The data of XRBs in quiescent state.**

Name	$d_L$ kpc	$L_X^{2-10\text{keV}}$ log(ergs/s)	$L_R^{5\text{GHz}}$ log(ergs/s)	$M_{\text{BH}}$ log( $M_\odot$ )	$\frac{L_X}{L_{\text{Edd}}}$	$\frac{L_{X,c}}{L_{\text{Edd}}}$	Ref. <sup>a</sup>
XTE J1752-223	3.5	32.80	27.71	0.99	-6.30	-5.52	1, 2, 2, 1
H1743-322	7.5	33.00	28.35	1.12	-6.23	-5.55	3, 4, 4, 5
XTE J1118+480	1.7	30.52	25.92	0.88	-8.47	-5.51	6, 7, 7, 7
A0620-00	1.2	30.30	26.85	0.82	-8.63	-5.50	6, 8, 8, 9
V404 Cyg	7.5	31.98	27.97	1.08	-7.21	-5.54	10, 8, 8, 9
V404 Cyg	7.5	33.69	28.75	1.08	-5.50	-5.54	10, 8, 8, 9

<sup>a</sup> The reference for distance, X-ray luminosity, radio luminosity and BH mass respectively, which are shown as follows: 1)Shaposhnikov et al. (2010); 2)Ratti et al. (2012); 3)Jonker et al. (2010); 4)Coriat et al. (2011); 5)Russell et al. (2013); 6)Russell et al. (2006); 7)Gallo et al. (2014); 8)Fender et al. (2010); 9)Zhang (2013); 10)Miller-Jones et al. (2009).

**Table 2. The data of LLAGNs.**

Name	$L_X^{2-10\text{keV}}$ log(ergs/s)	$L_R^{5\text{GHz}}$ log(ergs/s)	$M_{\text{BH}}$ log $M_\odot$	Refs.	$\frac{L_X}{L_{\text{Edd}}}$	$\frac{L_{X,c}}{L_{\text{Edd}}}$	Name	$L_X^{2-10\text{keV}}$ log(ergs/s)	$L_R^{5\text{GHz}}$ log(ergs/s)	$M_{\text{BH}}$ log( $M_\odot$ )	Refs.	$\frac{L_X}{L_{\text{Edd}}}$	$\frac{L_{X,c}}{L_{\text{Edd}}}$
$L_X \gtrsim L_{X,c}$													
NGC 266	40.88	37.95	8.37	1,2,3	-5.60	-6.78	NGC 4203	39.69	36.70	7.79	1,2,3	-6.21	-6.68
NGC 2768	39.46 <sup>a</sup>	37.39	7.94	4,2,3	-6.12	-6.71	NGC 4235	42.25	37.62	7.60	1,5,3	-3.46	-6.65
NGC 3031	39.38	36.03	7.73	1,5,3	-6.46	-6.67	NGC 4258	40.89	35.78	7.57	1,5,3	-4.79	-6.64
NGC 3147	41.87	37.91	8.29	1,2,3	-4.53	-6.77	NGC 4395	39.58	34.59	4.63	1,2,3	-3.16	-6.14
NGC 3169	41.05	37.19	8.01	1,2,3	-5.07	-6.72	NGC 4450	40.02	36.78	7.40	1,2,3	-5.49	-6.61
NGC 3226	39.99	37.20	8.06	1,2,3	-6.18	-6.73	NGC 4477	39.60	35.64	7.89	1,5,3	-6.40	-6.70
NGC 3227	41.70	36.31	7.41	1,2,3	-3.82	-6.62	NGC 4548	39.74	36.55 <sup>c</sup>	7.08	1,10,3	-5.45	-6.56
NGC 3516	42.39	37.28	7.94	1,2,3	-3.66	-6.71	NGC 4565	39.56	36.26	7.41	1,2,3	-5.96	-6.62
NGC 3718	40.44	36.96	7.69	1,6,3	-5.36	-6.66	NGC 4579	41.15	37.55	7.77	1,2,3	-4.73	-6.68
NGC 3884	41.89	37.94 <sup>b</sup>	8.19	1,7,3	-4.41	-6.75	NGC 4594	40.69	37.85	8.46	1,11,3	-5.88	-6.79
NGC 3941	39.27	35.61	7.37	1,5,3	-6.21	-6.61	NGC 4639	40.18	35.40	6.77	1,5,3	-4.70	-6.51
NGC 3998	41.57	38.36	8.89	8,2,3	-5.43	-6.87	NGC 4772	39.30	36.48	7.57	1,2,3	-6.38	-6.64
NGC 4138	40.11	36.13	7.19	1,5,3	-5.19	-6.58	NGC 5033	40.70	36.94	7.60	1,5,3	-5.01	-6.65
NGC 4143	40.03	37.18	8.16	1,2,3	-6.24	-6.74	NGC 5548	43.23	37.89	8.81	1,5,3	-3.69	-6.85
NGC 4168	39.87	36.63	7.97	9,2,3	-6.21	-6.71	NGC 7626	40.97	38.48	8.71	1,2,3	-5.85	-6.84
$L_X \lesssim L_{X,c}$													
NGC 404	37.02	33.50	5.16	1,12,5	-6.25	-6.23	NGC 4459	38.87	36.09	7.82	1,11,3	-7.06	-6.69
NGC 821	38.30	35.40	8.21	13,13,3	-6.90	-6.75	NGC 4501	38.89	36.28	7.79	1,5,3	-7.01	-6.68
NGC 2787	38.79	37.01	8.14	1,2,3	-7.46	-6.74	NGC 4552	39.49	38.35	8.55	1,6,3	-7.17	-6.81
NGC 2841	38.26	36.00 <sup>c</sup>	8.31	1,10,3	-8.16	-6.77	NGC 4636	39.38	36.76 <sup>c</sup>	8.14	1,10,3	-6.87	-6.74
NGC 3245	39.29	36.98	8.21	1,11,3	-7.03	-6.75	NGC 4649	38.10	37.48 <sup>d</sup>	9.07	1,11,3	-9.08	-6.90
NGC 3379	37.53	35.73	8.18	1,11,3	-8.76	-6.75	NGC 4698	38.69	35.59	7.57	1,5,3	-6.99	-6.64
NGC 3607	38.63	37.01	8.40	1,14,3	-7.88	-6.78	NGC 4736	38.48	35.51 <sup>c</sup>	7.05	1,10,3	-6.68	-6.55
NGC 3627	37.60	36.11	7.24	12,15,3	-7.81	-6.60	NGC 4762	38.26	36.58 <sup>c</sup>	7.63	1,10,3	-7.48	-6.65
NGC 3628	38.24	36.13 <sup>c</sup>	7.24	1,10,3	-7.11	-6.59	NGC 5846	39.65	36.73	8.43	1,2,3	-6.89	-6.79
NGC 4216	38.91	36.58 <sup>c</sup>	8.09	1,10,3	-7.29	-6.73	NGC 5866	38.60	37.07	7.81	1,2,3	-7.32	-6.68
NGC 4278	39.64	37.95	8.61	1,6,3	-7.08	-6.82	Sgr A*	33.34	32.50	6.41 <sup>e</sup>	16,16,16	-11.18	-6.45

Note: a) The 0.3-7keV X-ray flux is converted to 2-10keV flux by assuming a power law spectrum with  $\Gamma = 2$  (see also, Miller et al. (2012))

b) The 5 GHz radio core emission of NGC 3884 is observed by MERLIN, operated by Jodrell Bank Observatory with resolution of  $\sim 0.5''$ ;

c) The 5 GHz radio luminosity is extrapolated from 15 GHz by assuming  $f_\nu \propto \nu^{-0.5}$  (e.g., Ho & Ulvestad 2001 and Ho 2002);

d) The 5 GHz radio core emission of NGC 4649 is extrapolated from 1.5 GHz;

e) The BH mass of Sgr A\* is estimated from stellar kinematics;

References for radio luminosity, X-ray luminosity and BH mass: 1) Ho (2009); 2) Nagar et al. (2005); 3) Ho et al. (2009); 4) Boroson et al. (2011); 5) Ho & Ulvestad (2001); 6) Nagar et al. (2001); 7) Filho et al. (2006); 8) Younes et al. (2011); 9) Panessa et al. (2006); 10) Nagar et al. (2002); 11) Ho (2002); 12) Yuan et al. (2009); 13) Pellegrini et al. (2007); 14) Fabbiano et al. (1989); 15) Laurent-Muehleisen et al. (1997); 16) Merloni et al. (2003);

5 GHz assuming a typical radio spectral index of  $\alpha = -0.12$  ( $F_\nu \propto \nu^{-\alpha}$ , e.g., Corbel et al. 2013) and it is the same case for X-ray luminosity by assuming a typical photon index of  $\Gamma = 1.6$  in LH state. The distance, BH mass, X-ray luminosity, radio luminosity and critical Eddington ratio of quiescent XRB are reported in

Table 1, where radio and X-ray luminosities for LH state of XRBs can be found in above references.

For supermassive BH sources, we select a sample from a Palomar Survey of nearby galaxies, which is a magnitude-limited spectroscopic study of a nearly complete sample of 486 bright ( $B_T \leq 12.5$  mag) northern ( $\delta > 0^\circ$ ) galaxies (see Ho et al.

**Table 3. The data of FR Is.**

Name	$L_X^{2-10\text{keV}}$ log(ergs/s)	$L_R^{5\text{GHz}}$ log(ergs/s)	$M_{\text{BH}}$ log( $M_\odot$ )	Refs.	$\frac{L_X}{L_{\text{Edd}}}$	$\frac{L_{X,c}}{L_{\text{Edd}}}$	Name	$L_X^{2-10\text{keV}}$ log(ergs/s)	$L_R^{5\text{GHz}}$ log(ergs/s)	$M_{\text{BH}}$ log( $M_\odot$ )	Refs.	$\frac{L_X}{L_{\text{Edd}}}$	$\frac{L_{X,c}}{L_{\text{Edd}}}$
$L_X \gtrsim L_{X,c}$													
3C 31	40.67	39.45	8.70	1,1,2	-6.14	-6.84	3C 442A	41.10	38.21	8.40	1,1,6	-5.41	-6.78
3C 66B	41.10	39.97	8.84	1,1,2	-5.85	-6.86	3C 449	40.35	39.08	8.54	1,1,2	-6.30	-6.81
3C 76.1	41.28	39.07	8.08	1,1,3	-4.95	-6.74	3C 465	41.04	40.41	9.13	1,1,2	-6.20	-6.91
3C 83.1B	41.13	39.46	9.01	1,1,2	-5.99	-6.89	NGC 315	41.63	40.41	8.89	7,8,9	-5.37	-6.87
3C 84	42.91	42.32	8.64	1,4,2	-3.84	-6.82	NGC 507	40.66	37.67	8.91	7,10,9	-7.12	-6.87
3C 264	41.87	39.98	8.61	1,5,2	-5.04	-6.85	NGC 1052	41.53	39.85	8.25	7,11,9	-4.83	-6.76
3C 296	41.49	39.68	8.80	1,1,2	-5.42	-6.85	NGC 4261	40.59	39.21	8.92	7,8,9	-6.44	-6.87
3C 305	41.42	39.75	8.10	1,1,2	-4.79	-6.73	NGC 6109	40.35	39.44	8.56	1,1,2	-6.31	-6.81
3C 338	40.31	40.03	8.92	1,1,2	-6.73	-6.87	NGC 6251	41.60	40.35 <sup>a</sup>	8.97	6,1,2	-5.48	-6.88
3C 346	43.40	41.83	8.89	1,1,2	-3.60	-6.87							
$L_X \lesssim L_{X,c}$													
3C272.1	39.35	38.22	8.80	1,1,2	-7.56	-6.85	3C274	40.59	39.87	9.48	1,1,2	-7.00	-6.97

Note:<sup>a</sup>: the radio luminosity is derived from the observation of VLBI.

References: 1) Hardcastle et al. (2009); 2) Wu et al. (2011); 3) Woo et al. (2002); 4) Laurent-Muehleisen et al. (1997); 5) Lara et al. (2004); 6) Wu et al. (2013); 7) Ho (2009); 8)Merloni et al. (2003); 9) Ho et al. (2009); 10) Murgia et al. (2011); 11) Fabbiano et al. (1989)

1997a,b for more details, and references therein). The nuclear X-ray luminosities and central stellar velocity dispersions for the sources in this survey are further given in Ho (2009) and Ho et al. (2009) respectively, where the sources observed by *Chandra* and/or *XMM – Newton* are selected in this work. For our purpose, we exclude the sources with only upper limit of X-ray luminosity and the sources with  $L_X > 10^{-3}L_{\text{Edd}}$  which may stay in radiatively efficient phase (e.g., Ho 2008). The radio core emission of these sources is selected (e.g., Ho & Ulvestad 2001; Nagar et al. 2001, 2005; Filho et al. 2006), where most of sources are observed by Very Large Array (VLA, at resolution of  $\sim 1''$ ) or even Very Long Baseline Array (VLBA) at higher resolution and NGC 3884 observed by MERLIN is also selected. The radio fluxes of 7 sources observed by VLA at 15 GHz are converted to 5 GHz by assuming  $F_\nu \propto \nu^{-\alpha}$  ( $\alpha = 0.5$  is adopted, e.g., Ho & Peng 2001; Ho 2002). The fifteen putative Compton-thick sources are also neglected (NGC 1068, NGC 676, NGC 1167, NGC 1667, NGC 2273, NGC 3185, NGC 3489, NGC 3982, NGC 5194, NGC 7743 (Panessa et al. 2006) Mrk 3, NGC 4945, NGC 7479 (Georgantopoulos et al. 2011) and NGC 2655, NGC 2639 (Terashima, et al. 2005), since that the X-ray and other band emission may be seriously obscured. The BH mass of selected sources is calculated from the  $M_{\text{BH}} - \sigma_*$  relation of Gültekin et al. (2009b),

$$\log \frac{M_{\text{BH}}}{M_\odot} = (8.12 \pm 0.08) + (4.24 \pm 0.41) \log \frac{\sigma_*}{200 \text{ km s}^{-1}} \quad (4)$$

where  $\sigma_*$  is selected from Ho et al. (2009). The famous supermassive BH in our Galactic center (Sgr A\*, the quiescent state) is also included even it was not included in Palomar sample. We note that Palomar sample include several traditionally radio-loud sources with relativistic large-scale jets (e.g., NGC 315, NGC 507, NGC 1275, NGC 4261, NGC 4374 and NGC 4486), where the central engine may be different from those without relativistic jets. To explore the radio–X-ray correlation in these strong radio sources and compare it with that of Yuan et al. (2009), we select 17 more FR Is with relativistic jets from 3CRR sample. Similar to LLAGN sample, the selected FR Is should be observed by *Chandra/XMM – Newton* in X-ray band and VLA/VLBA at radio waveband. The radio core emission of these FR Is is adopted

in this work. The BH mass are also calculated from their central stellar velocity dispersions (Ho 2009; Wu et al. 2011). In total, we select 52 LLAGNs without evident relativistic large-scale jets (22 sources have  $L_X < L_{X,c}$ ) and 21 FR Is with strong jets (2 sources have  $L_X < L_{X,c}$ ), which are listed in Tables (2) and (3) respectively, where the X-ray luminosity, radio luminosity and BH mass for each selected source are reported.

### 3 METHOD AND RESULT

To explore the fundamental plane for the sub-Eddington and quiescent BHs, we take the form of  $\log L_R = \xi_X \log L_X + \xi_M \log M_{\text{BH}} + c_0$  as in Merloni et al. (2003), where  $L_R$  is 5 GHz radio luminosity,  $L_X$  is 2-10 keV X-ray luminosity. To find the multi-parameter relation, we adopt a similar approach as that of Merloni et al. (2003) and minimize the following statistic,

$$\chi^2 = \sum_i \frac{(y_i - c_0 - \xi_X X_i - \xi_M M_i)^2}{\sigma_R^2 + \xi_X^2 \sigma_X^2 + \xi_M^2 \sigma_M^2}, \quad (5)$$

where  $y_i = \log L_R$ ,  $X_i = \log L_X$ ,  $M_i = \log M_{\text{BH}}$  and  $c_0$  is a constant. Instead of assuming the isotropic uncertainties with  $\sigma_{L_R} = \sigma_{L_X} = \sigma_M$  as in Merloni et al. (2003), we adopt the typical observational uncertainties  $\sigma_{L_R} = 0.2$  dex (e.g., Ho & Peng 2001),  $\sigma_{L_X} = 0.3$  dex (e.g., Strateva et al. 2005), and  $\sigma_M = 0.4$  dex (e.g., Vestergaard & Peterson 2006) for AGNs and the typical variations (within one day)  $\sigma_{L_R} = 0.1$  dex,  $\sigma_{L_X} = 0.15$  dex (e.g., Coriat et al. 2011; Corbel et al. 2013), and typical uncertainty of BH mass  $\sigma_M = 0.15$  dex (e.g., Zhang 2013) for XRBs.

In top-left panel of Figure 1, we present the fundamental plane for all selected BH sources from sub-Eddington to quiescent state. The best fit for the whole sample is

$$\log L_R = 0.55^{+0.19}_{-0.17} \log L_X + 0.80^{+0.16}_{-0.13} \log M_{\text{BH}} + 9.17^{+0.34}_{-0.34}, \quad (6)$$

with an intrinsic scatter of  $\sigma_{\text{int}} = 0.36$  dex. From this panel, we find (1) the quiescent BHs still roughly follow the correlation as defined by the whole sample and do not show evident deviation; (2) the FR Is seem to follow a steeper track comparing with other

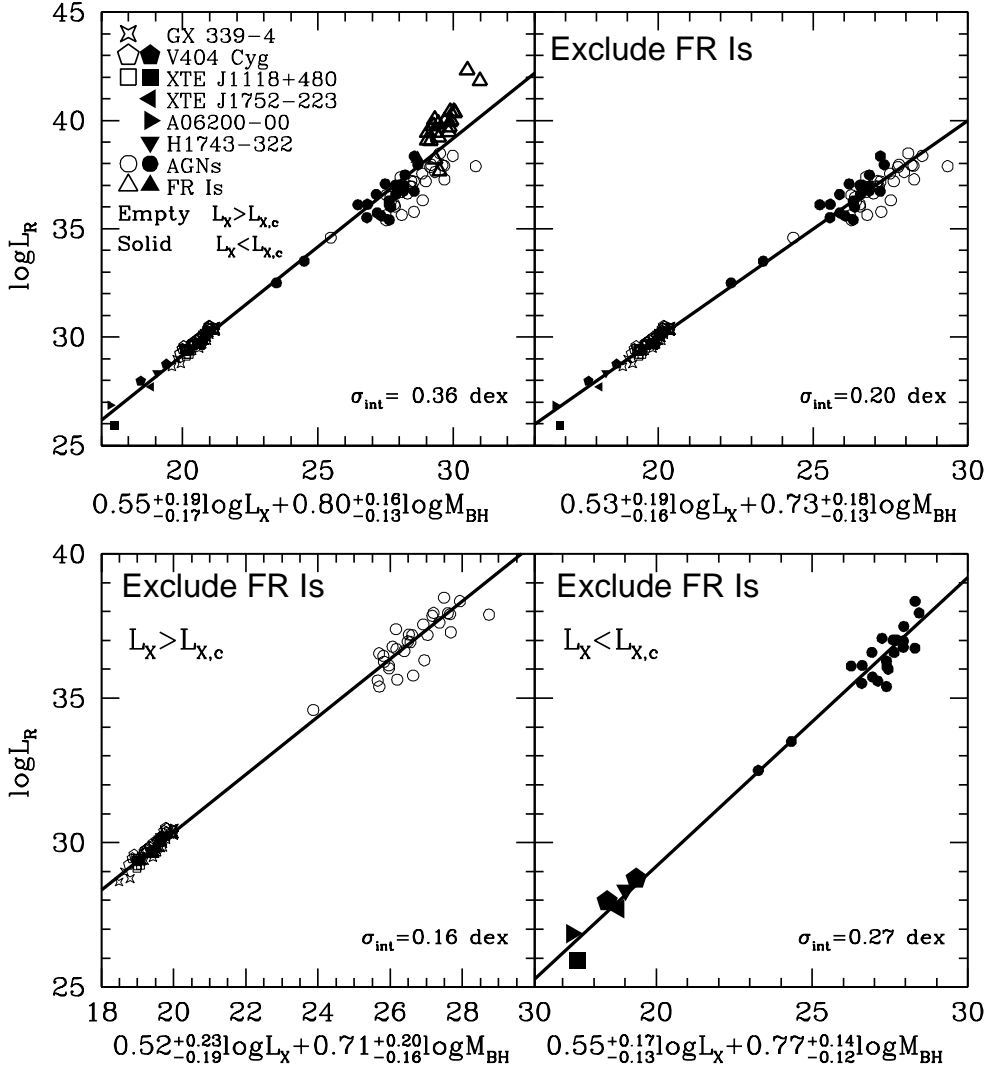


**Figure 1.** The fundamental plane for the BH activities, where the empty and solid points represent the sources with  $L_X < L_{X,c}$  and  $L_X > L_{X,c}$  respectively. Top-left panel represent the plane for all BH sources as selected in our sample; Top-right panel represent the plane for BH sources after excluding FR Is; Bottom panels represent the plane for BHs (exclude FR Is) with  $L_X > L_{X,c}$  (left) and  $L_X < L_{X,c}$  (right) respectively. The solid lines are the best fittings.

sources. After excluding the FR Is from the whole sample, we present the fundamental plane for other sources in top-right panel of Figure 1 and the best fit is

$$\log L_R = 0.52^{+0.23}_{-0.19} \log L_X + 0.73^{+0.18}_{-0.13} \log M_{\text{BH}} + 9.97^{+0.31}_{-0.30}, \quad (7)$$

with an intrinsic  $\sigma_{\text{int}} = 0.20$  dex. It can be found that the fundamental plane becomes a little bit tighter after removing FR I sources, even the slope of  $\xi_X$  is roughly unchanged.

We further divide the sample (excluding FR Is) into two subsamples with  $L_X > L_{X,c}$  (sub-Eddington sources) and  $L_X < L_{X,c}$  (quiescent sources) respectively, where the fundamental planes are shown in bottom-left and bottom-right panels of Figure 1 respectively. The best fit for sources with  $L_X > L_{X,c}$  is

$$\log L_R = 0.53^{+0.23}_{-0.19} \log L_X + 0.71^{+0.20}_{-0.16} \log M_{\text{BH}} + 10.36^{+0.29}_{-0.28}, \quad (8)$$

with an intrinsic  $\sigma_{\text{int}} = 0.16$  dex. The best fit for sources with  $L_X < L_{X,c}$  is

$$\log L_R = 0.55^{+0.17}_{-0.13} \log L_X + 0.77^{+0.14}_{-0.12} \log M_{\text{BH}} + 9.17^{+0.44}_{-0.44}, \quad (9)$$

with an intrinsic  $\sigma_{\text{int}} = 0.27$  dex.

To investigate the radio–X-ray correlation and eliminate the mass effect in AGNs, we further select sources with BH mass in a narrow range but with a broad range of Eddington ratios, which can be used to simulate a single supermassive BH evolving from LH state to quiescent state in a statistical manner. Due to the evident differences in the slope of radio–X-ray correlation for FR Is and other LLAGNs, we explore this issue for these two populations separately (their BH mass distributions are also much different). We select 28 LLAGNs from Table (1), which have BH mass  $M_{\text{BH}} = 10^{8 \pm 0.4} M_{\odot}$  and Eddington ratios of  $L_{2-10\text{keV}}/L_{\text{Edd}} \sim 10^{-8.8}$  to  $10^{-3}$ . The result is shown in Figure 2, where the faintest sources with  $L_X \lesssim L_{X,c}$  (solid circles) roughly follow the trend of other sub-Eddington sources. The best-fit linear regression for all sources yields

$$\log L_R = 0.49 \pm 0.04 \log L_X + 17.53 \pm 1.64, \quad (10)$$

with a Spearman correlation coefficient of  $r = 0.75$  and  $p = 2.41 \times 10^{-11}$ , where the linear regressions were not given for sources with  $L_X > L_{X,c}$  and  $L_X \lesssim L_{X,c}$  respectively due to the narrow range and large scatter of the data in each population. A

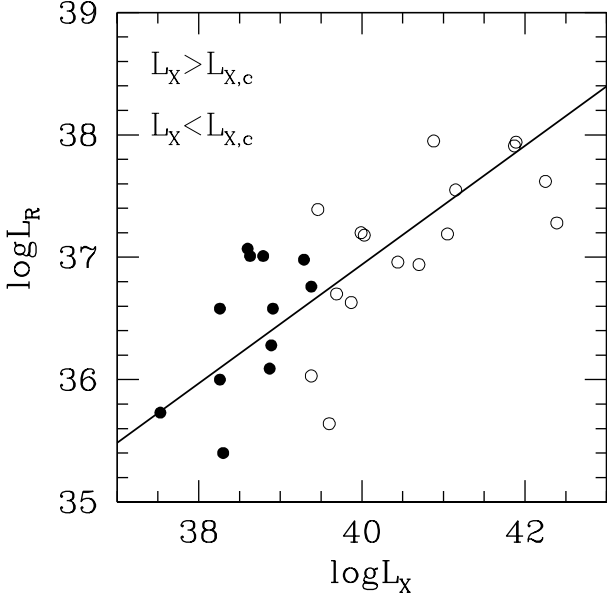


**Figure 2.** The relation between 5 GHz radio and 2-10 keV X-ray luminosities for LLAGNs with BH mass within  $10^{8.8 \pm 0.4} M_{\odot}$ , where solid and empty circles represent the sources with  $L_X > L_{X,c}$  and  $L_X < L_{X,c}$  respectively. The solid line is the best fitting for all sources.

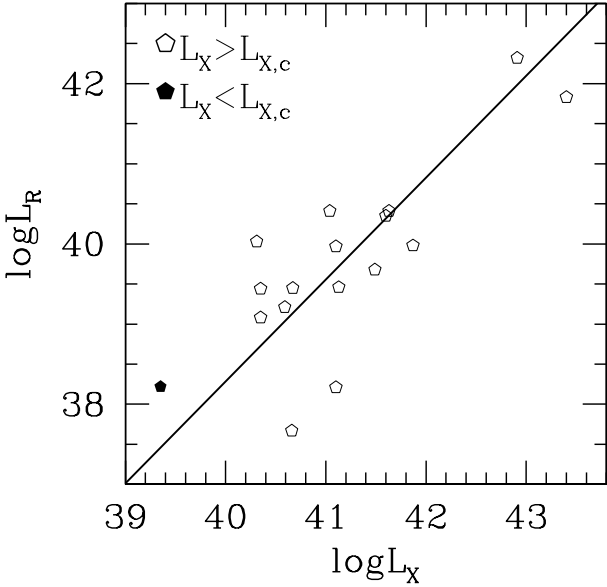


**Figure 3.** The same as Figure 2, but for FR Is with BH mass within  $M_{\text{BH}} = 10^{8.8 \pm 0.4}$ .

similar analysis was also done for 14 FR Is with BH mass within  $10^{8.8 \pm 0.4} M_{\odot}$  and  $L_{2-10\text{keV}}/L_{\text{Edd}}$  range from  $10^{-7.6}$  to  $10^{-3.6}$ . The radio–X-ray correlation of these FR Is is shown in Figure 3, and the best fit is

$$\log L_{\text{R}} = 1.27 \pm 0.10 \log L_{\text{X}} - 12.56 \pm 3.97, \quad (11)$$

with a Spearman correlation coefficient of  $r = 0.80$  and  $p = 3.44 \times 10^{-13}$ .

## 4 CONCLUSION AND DISCUSSION

In this work, we reinvestigate the radio–X-ray correlation and the fundamental plane of BH activity for a sample of XRBs and LLAGNs from sub-Eddington to quiescent state after including more quiescent BHs. The main results are summarized as follows: 1) the fundamental plane for the quiescent BHs is similar to that of sub-Eddington sources and do not show evident differences; 2) the radio loud AGNs (e.g., FR Is) follow a separate and steeper radio–X-ray correlation comparing with other BH sources; 3) the radio–X-ray correlation can roughly extend to quiescent BHs with  $L_{2-10\text{keV}}/L_{\text{Edd}} \sim 10^{-8.8}$  in LLAGNs and  $L_{2-10\text{keV}}/L_{\text{Edd}} \sim 10^{-7.6}$  in FR Is, where both subsamples have BH mass in a narrow range that can simulate a single supermassive BH evolving from sub-Eddington to quiescent state. These results are similar to that of XRBs where the quiescent XRBs with  $L_{2-10\text{keV}}/L_{\text{Edd}} < 10^{-8.5}$  still follow the radio–X-ray correlation as defined in LH state (Gallo et al. 2006, 2014, for A0620-00 and XTE J1118+480).

The radio–X-ray correlation plays an important role in understanding the physics of BH central engines, which was widely explored in XRBs and AGNs. It is roughly consensus that faint BHs with  $L_{\text{bol}}/L_{\text{Edd}} \lesssim 1\%$  follow a shallower radio–X-ray correlation with  $\xi_{\text{X}} \sim 0.5 - 0.7$  (e.g., Corbel et al. 2003; Gallo et al. 2003; Corbel et al. 2013) while brighter BHs with  $L_{\text{bol}}/L_{\text{Edd}} \gtrsim 1\%$  follow a steeper track with  $\xi_{\text{X}} \sim 1.2 - 1.6$  (e.g., Coriat et al. 2011; Dong et al. 2014; Panessa et al. 2015). However, it is still debatable whether the quiescent BHs still follow the radio–X-ray correlation with  $\xi_{\text{X}} \sim 0.5 - 0.7$  as defined in LH state of XRBs or not. Yuan et al. (2009) found the LLAGNs with  $L_X \lesssim L_{X,c} \sim 10^{-6} - 10^{-5} L_{\text{Edd}}$  follow a steeper radio–X-ray correlation (e.g.,  $L_{\text{R}} \propto L_X^{1.22}$ ), which is roughly consistent with their model prediction in Yuan & Cui (2005) where the X-ray emission switches from being ADAF to jet dominated. However, several quiescent XRBs challenge this conclusion where the sources with  $L_X \lesssim 10^{-8.5} L_{\text{Edd}}$  still follow the radio–X-ray correlation as defined by LH state of XRBs very well (e.g., A0620-00, Gallo et al. 2006 and XTE J1118+480, Gallo et al. 2014). We further explore this issue using a large sample of BHs from highly sub-Eddington to sub-Eddington. We don’t find that the quiescent BHs with  $L_X < L_{X,c}$  are different from other sub-Eddington BHs based on the analysis of the radio–X-ray correlation and the fundamental plane. In particular, we also use two subsamples with similar BH mass (FR Is with  $M_{\text{BH}} = 10^{8.8 \pm 0.4}$  and other LLAGNs with  $M_{\text{BH}} = 10^{8.0 \pm 0.4}$ ) to simulate the behavior of a single supermassive BH evolving across from sub-Eddington to quiescent state (e.g., LLAGNs have  $L_X \sim 10^{-9} - 10^{-3} L_{\text{Edd}}$  and FR Is have  $L_X \sim 10^{-7.6} - 10^{-3.6} L_{\text{Edd}}$ ). The quiescent BHs still roughly follow that defined by the whole sample. Our results are consistent with that of XRBs (Gallo et al. 2006, 2014), but is different from that derived from AGNs (Yuan et al. 2009). The possible reason is that BH sources observed with large-scale relativistic jets (e.g., FR Is) are included in Yuan et al. (2009)’s sample, where RL AGNs normally follow a much steeper radio–X-ray correlation regardless of Eddington ratios (see also  $L_{\text{R}} \propto L_X^{1.5}$ , Li et al. 2008; de Gasperin et al. 2011 or FR I sample in this work). The bimodal distribution of radio loudness in AGNs is still an open issue. From the slope of radio–X-ray correlation, we can find that the normal LLAGNs may be similar to LH state of XRBs while RL FR Is with relativistic jets may be intrinsically different. However, it should be noted that the intrinsic correlation may be different comparing with the observed radio–X-ray in RL AGNs, where the Doppler boosting effect is not considered in our work (also Li et al. 2008; Yuan et al.

2009; de Gasperin et al. 2011) which may correlate with the luminosities (e.g., Kang et al. 2014). Better constraints on the Doppler factors in both XRBs and AGNs are expected to further investigate this issue. It should be also noted that our subsample with similar BH mass is still limited. More sources with similar BH mass and a wide distribution of Eddington ratio are expected to further test the possible radio–X-ray correlation from quiescent to sub-Eddington BHs.

The radio emission is normally believed to originate from the jet in both XRBs and AGNs. The radio–X-ray correlation in BH systems suggests the possible coupling of disc and jet, where the X-ray emission dominantly comes from ADAF or corona (but see Markoff et al. 2005, for a different opinion). The origin of X-ray emission from sub-Eddington to quiescent BHs may not change (e.g., ADAF or jet) if the radio–X-ray as found in LH state of XRBs can extend to quiescent state. Yuan & Cui (2005) predicted that the radio–X-ray correlation will become steeper if  $L_X \lesssim L_{X,c}$  and the data points will stay below the radio–X-ray correlation as defined in LH state, where the origin of X-ray emission switches from being ADAF to jet dominated. If this is the real case, the observational results suggest that the critical X-ray luminosity may be lower than that reported in Yuan & Cui (2005), where there are still many uncertainties in the ADAF-jet model. In modeling the SED of quiescent BHs with ADAF-jet model, Xie et al. (2014) suggested that the X-ray emission of V404 Cyg in quiescent state should be dominated by jet based on its X-ray shape (see also Yuan et al. 2009, for a couple of quiescent supermassive BHs), where jet produce power-law X-ray spectrum while the inverse-Compton spectrum from ADAF is normally curved. The soften of X-ray spectrum in quiescent BHs can be explained by both ADAF and jet models separately, where the bremsstrahlung radiation will contribute to X-ray emission (Esin et al. 1997) while the synchrotron emission normally produce a power-law X-ray with  $\Gamma \sim 2$  (e.g., Yuan et al. 2009; Xie et al. 2014; Yang et al. 2015). Broadband X-ray observation in quiescent BHs and better dealing with Comptonization in ADAF are expected to further test this issue.

The RL AGNs normally follow a steeper radio–X-ray correlation (e.g., FR Is, see also Li et al. 2008; de Gasperin et al. 2011). The physical reason for steeper correlation as found in FR Is is unclear, which may include: 1) the origin of the X-ray emission is different, where the X-ray come from accretion flows in RQ LLAGNs while it is, similar to radio, come from the jet in RL FR Is (e.g., Hardcastle et al. 2009); 2) X-ray emission always come from the jet for both RQ AGNs and RL AGNs, but the effect of jet synchrotron cooling is depend on BH mass, where most of the RL FR Is have more massive BHs (e.g.,  $M_{BH} \gtrsim 10^8 \odot$ ) and may follow a steeper radio-X-ray correlation that regulated by synchrotron cooling in the jet (e.g., Plotkin et al. 2013); 3) different accretion-jet properties, where the stronger radio jet in FR Is may be regulated by a rapidly rotating BH while the radio emission of radio weak AGNs is dominated by weak jets or disk winds (Wu et al. 2011). Better constraints on the origin of X-ray emission and/or the possible correlation between jet and BH spin for more sources may shed light on this issue. Furthermore, a more uniform and larger sample with wider distributions of radio loudness and Eddington ratio is wished to further explore the possible ‘fundamental plane’.

## ACKNOWLEDGMENTS

We thank HUST astrophysics group for many useful discussions and comments. This work is supported by the NSFC (grants

11103003, 11133005, 11573009 and 11303010) and New Century Excellent Talents in University (NCET-13-0238).

## REFERENCES

- Abramowicz M. A., Chen X., Kato S., et al., 1995, *ApJ*, 438, L37  
 Boroson B., Kim D.-W., Fabbiano G., 2011, *ApJ*, 729, 12  
 Cadolle Bel, M., Ribó M., Rodriguez, J., et al., 2007, *ApJ*, 659, 549  
 Cao, X.-F., Wu, Q., & Dong, A.-J. 2014, *ApJ*, 788, 52  
 Cao, X. 2009, *MNRAS*, 394, 207  
 Cao, X., Wang, J.-X. 2015, *MNRAS*, in press (arXiv:1406.6442)  
 Calvelo, D. E., et al. 2010, *MNRAS*, 409, 839  
 Constantin, A., Green, P., Aldcroft, T., Kim, D.-W., Haggard, D., Barkhouse, W., Anderson, S. F. 2009, *ApJ*, 705, 1336  
 Corbel S., Nowak M. A., Fender R. P., et al., 2003, *A&A*, 400, 1007  
 Corbel S., Coriat M., Brocksopp C., et al., 2013, *MNRAS*, 428, 2500  
 Coriat M., Corbel S., Prat L., et al., 2011, *MNRAS*, 414, 677  
 de Gasperin, F., Merloni, A., Sell, P., Best, P., Heinz, S., Kauffmann, G. 2011, *MNRAS*, 415, 2910  
 Dong, A. -J., Wu, Q., Cao, X. -W. 2014, *ApJ*, 787, 20  
 Esin, A. A., McClintock, J. E., Narayan, R. 1997, *ApJ*, 489, 865  
 Fabbiano, G., Gioia, I. M., Trinchieri, G., 1989, *ApJ*, 347, 127  
 Falcke H., Körding E., Markoff S., 2004, *A&A*, 414, 895  
 Fender, R. P., Gallo, E., Russell, D. 2010, *MNRAS*, 406, 1425  
 Filho M. E., Barthel P. D., Ho L. C., 2006, *A&A*, 451, 71  
 Gallo E., Fender R. P., Pooley G. G., 2003, *MNRAS*, 344, 60  
 Gallo, E., Fender, R. P., Miller-Jones, J. C. A., Merloni, A., Jonker, P. G., Heinz, S., Maccarone, T. J., van der Klis, M., 2006, *MNRAS*, 370, 1351  
 Gallo E., et al. 2014, *MNRAS*, 445, 290  
 Georgantopoulos, I., et al. 2011, *A&A*, 534, 23.  
 Gu, M., Cao, X. 2009, *MNRAS*, 399, 349  
 Gültekin K., Cackett E. M., Miller J. M., et al., 2009, *ApJ*, 706, 404  
 Gültekin K., et al., 2009, *ApJ*, 698, 198  
 Hannikainen D. C., Hunstead R.-W., Campbell-Wilson D., Sood R. K., 1998, *A&A*, 337, 460  
 Hardcastle, M. J., Evans, D. A., Croston, J. H., 2009, *MNRAS*, 396, 1929  
 Ho, L. C. 2009, *ApJ*, 699, 626  
 Ho, L. C., Greene, J. E., Filippenko, A. V., Sargent, W. L. W., 2009, *ApJS*, 183, 1  
 Ho, L. C. 2008, *ARA&A*, 46, 475  
 Ho, L. C. 2002, *ApJ*, 564, 120  
 Ho, L. C., & Ulvestad, J. S. 2001, *ApJs*, 133, 77  
 Ho, L. C., & Peng, C. Y. 2001, *ApJ*, 555, 650  
 Ho, L. C., Filippenko, A. V., & Sargent, W. L. W. 1997a, *ApJS*, 112, 315  
 Ho, L. C., Filippenko, A. V., & Sargent, W. L. W. 1997b, *ApJ*, 487, 568  
 Ivezić, Z., et al. 2002, *AJ*, 124, 2364  
 Huang, C.-Y., Wu, Q., Wang, D.-X., 2014, *MNRAS*, 440, 965  
 Ichimaru S., 1977, *ApJ*, 214, 840  
 Jang, I., Gliozzi, M., Hughes, C., Titarchuk, L., 2014, *MNRAS*, 443, 72  
 Jonker P. G., Miller-Jones J., Homan J., 2010, *MNRAS*, 401, 1255  
 Kang, S.-J., Chen, L. & Wu, Q. 2014, *ApJS*, 215, 5  
 Körding, E. G., Jester, S., Fender, R. 2006a, *MNRAS*, 372, 1266

- Körding E., Falcke H., Corbel S., 2006b, *A&A*, 456, 439  
 Laurent-Muehleisen, S. A., et al., 1997, *A&AS*, 122, 235  
 Li Z.-Y., Wu X.-B., Wang R., 2008, *ApJ*, 688, 826  
 Liu, H., & Wu, Q. 2013, *ApJ*, 764, 17  
 Lara, L., Giovannini, G., Cotton, W. D., Feretti, L., Venturi, T., 2004, *A&A*, 415, 905  
 Markoff, S., Nowak, M. A., Wilms, J. 2005, *ApJ*, 635, 1203  
 McClintock J. E., Remillard R. A., 2006, in Lewin, van der Klis, eds, *Compact Stellar X-ray Sources*. Cambridge Univ. Press, Cambridge, p. 157  
 Merloni A., Heinz S., Matteo T. D., 2003, *MNRAS*, 345, 1057  
 Miller-Jones, J. C. A., et al. 2009 *MNRAS*, 394, 1440  
 Miller, B., Gallo, E., Treu, T., Woo, J.-H., 2012, *ApJ*, 747, 57  
 Murgia, M., et al., 2011, *A&A*, 526, 148  
 Narayan R., Yi I., 1994, *ApJ*, 428, L13  
 Narayan R., Yi I., 1995, *ApJ*, 444, 231  
 Nagar N. M., Falcke H., Wilson A. S., 2005, *A&A*, 435, 521  
 Nagar, N. M., Falcke, H., Wilson, A. S., Ulvestad, J. S., 2002, *A&A*, 392, 53  
 Nagar N. M., Wilson, A. S., Falcke H., 2001, *ApJ*, 559, 87  
 Panessa, F., et al. 2015, accepted by *MNRAS*, arXiv:1411.7829  
 Panessa, F., et al. 2006, *A&A*, 455, 173  
 Pellegrini, S., et al., 2007, *ApJ*, 667, 749  
 Plotkin, R. M., et al. 2015, *MNRAS*, 446, 4098  
 Plotkin, R. M., Gallo, E., Jonker, P. G. 2013, *ApJ*, 773, 59  
 Plotkin R. M., Markoff S., Kelly B. C., et al., 2012, *MNRAS*, 419, 267  
 Qiao, E., Liu, B. F. 2015, *MNRAS* in press  
 Qiao, E., Liu, B. F. 2013, *ApJ*, 764, 2  
 Ratti E. M., Jonker P. G., Miller-Jones J. A. C., et al., 2012, *MNRAS*, 423, 2656  
 Russell, D. M., Fender, R. P., Hynes, R. I., Brocksopp, C., Homan, J., Jonker, P. G., Buxton, M. M. 2006, *MNRAS*, 371, 1334  
 Russell, D. M., Gallo, E., Fender, R. P., 2013, *MNRAS*, 431, 405  
 Shaposhnikov N., Markwardt C., Swank J., Krimm H., 2010, *ApJ*, 723, 1817  
 Shakura N. I., Sunyaev R. A., 1973, *A&A*, 24, 337 (SS73)  
 Shemmer, O., Brandt, W. N., Netzer, H., Maiolino, R., Kaspi, S. 2008, *ApJ*, 682, 81  
 Sikora, M., Stawarz, L., Lasota, J.-P. 2007, *ApJ*, 658, 815  
 Soleri P., Fender R., Tudose V., et al., 2010, *MNRAS*, 406, 1471  
 Strateva, I. V., Brandt, W. N., Schneider, D. P., Vanden Berk, D. G., & Vignali, C. 2005, *AJ*, 130, 387  
 Terashima, Y., Ho, L. C., Ptak, A. F., 2000, *ApJ*, 539, 161  
 Urry, C. M., Padovani, P. 1995, *PASP*, 107, 803  
 Vestergaard, M., & Peterson, B. M. 2006, *ApJ*, 641, 689  
 Wang, J.-M., Watarai, K.-Y., Mineshige, S. 2004, *ApJ*, 607, 107  
 Wang R., Wu X.-B., Kong M.-Z., 2006, *ApJ*, 645, 890  
 White, R. L., et al. 2000, *ApJS*, 126, 133  
 Woo, J.-H., Urry, C. M., 2002, *ApJ*, 579, 530  
 Wu, Q., Cao, X. 2006, *PASP*, 118, 1098  
 Wu, Q., Gu, M. 2008, *ApJ*, 682, 212  
 Wu Q., Cao X., Wang D.-X., 2011, *ApJ*, 735, 50  
 Wu, Q., Cao, X., Ho, L. C., Wang, D.-X., 2013, *ApJ*, 770, 31  
 Xie, F.-G., Yang, Q.-X., Ma, R. 2014, *MNRAS*, 442, 110  
 Xue, Y. Q., Cui, W. 2007, *A&A*, 466, 1053  
 Yang, Q.-X., Xie, F.-G., Yuan, F., Zdziarski, A. A., Gierlinski, M., Ho, L. C., Yu, Z. 2015, *MNRAS*, 447, 1692  
 Yuan, F., Narayan, R., 2014, *ARA&A*, 52, 529  
 Yuan F., Yu Z., Ho L. C., 2009, *ApJ*, 703, 1034  
 Yuan, F., Quataert, E., & Narayan, R. 2003, *ApJ*, 598, 301  
 Yuan F., Cui W., 2005, *ApJ*, 629, 408  
 Younes, G., Porquet, D., Sabra, B., Reeves, J. N., 2011, *A&A*, 530, 149  
 Zhang, S.-N. 2013, *FrPhy*, 8, 630